Catalysts **2015**, *5*, 1846-1861; doi:10.3390/catal5041846

OPEN ACCESS

catalysts

ISSN 2073-4344

www.mdpi.com/journal/catalysts

Article

Catalytic Hydrogenation of CO_2 to Methanol: Study of Synergistic Effect on Adsorption Properties of CO_2 and H_2 in $CuO/ZnO/ZrO_2$ System

Chunjie Huang, Shaoyun Chen, Xiaoyao Fei, Dai Liu and Yongchun Zhang *

State Key Laboratory of Fine Chemistry, School of Chemical Engineering,
Dalian University of Technology, 116024 Liaoning, China;
E-Mails: huangchunjie@mail.dlut.edu.cn (C.H.); chen_shy@sina.com (S.C.);
dbchfxy@163.com (X.F.); liudai8936@126.com (D.L.)

* Author to whom correspondence should be addressed; E-Mail: zalidy5518@vip.sina.com;
Tel./Fax: +86-411-84986332.

Academic Editor: Keith Hohn

Received: 29 September 2015 / Accepted: 30 October 2015 / Published: 6 November 2015

Abstract: A series of $CuO/ZnO/ZrO_2$ (CZZ) catalysts with different CuO/ZnO weight ratios have been synthesized by citrate method and tested in the catalytic hydrogenation of CO_2 to methanol. Experimental results showed that the catalyst with the lowest CuO/ZnO weight ratio of 2/7 exhibited the best catalytic performance with a CO_2 conversion of 32.9%, 45.8% methanol selectivity, and a process delivery of 193.9 $g_{MeOH} \cdot kg_{cat}^{-1} \cdot h^{-1}$. A synergetic effect is found by systematic temperature-programmed-desorption (TPD) studies. Comparing with single and di-component systems, the interaction via different components in a CZZ system provides additional active sites to adsorb more H_2 and CO_2 in the low temperature range, resulting in higher weight time yield (WTY) of methanol.

Keywords: methanol synthesis; CO_2 conversion; synergetic effect; medium basic site; citrate method

1. Introduction

CO_2, as a major greenhouse gas, is significantly responsible for global warming (greenhouse effect) and climate changes in recent decades [1]. Technologies of capturing atmospheric CO_2 have recently

been developed, such as using efficient absorbents or exploring novel process and technologies based on "CO_2 sequestration" [2,3]. In addition to permanent storage and direct utilization as a solvent or working fluid, chemical conversion of CO_2 to useful chemicals, such as methanol (MeOH), is recently under increased scrutiny as an opportunity to be used as a low-cost carbon source [4].

MeOH was mainly used as a starting feedstock in the chemical industries. It could also be an efficient alternative and sustainable synthetic fuel if regenerative hydrogen and anthropogenic CO_2 are used as reagent for its synthesis. One way of accomplishing this goal is exploring highly active and selective catalysts for methanol synthesis, because of the thermodynamic stability of CO_2. Currently, a $Cu/ZnO/Al_2O_3$ catalyst system has been employed industrially in MeOH synthesis for over half a century (a worldwide demand of 75 Mtons·year^{-1}). It was run mostly at elevated pressures (5–10 MPa) and high temperature (493–573 K) by feeding a CO (5%)-CO_2 (5%)-H_2 syngas stream [5]. Although good conversion efficiency was obtained, such catalysts exhibited a poor reaction activity in pure CO_2 systems [6,7]. For the strong hydrophilic character of the alumina carrier, significant amounts of water forms and assembles on the catalyst during activation and reaction procedures. The water was found to inhibit CO_2 hydrogenation [8,9]. Importantly, methanol was shown to be a direct reaction product formed from CO_2 and not via CO [10–12]. A poisoning effect of water on active sites could explain the reduced functionality of alumina-based catalysts in CO_2-H_2 streams [13].

Recently, the $Cu/ZnO/ZrO_2$ (CZZ) system was reported to be more promising in providing a high MeOH yield compared with conventional methanol catalysts. Such catalyst systems have the unique properties of zirconium, such as the preservation of both acid and basic sites, the reducing and oxidizing properties, as well as high thermal stability [14]. Moreover, aiming to further enhance the reactivity of such CZZ systems, different oxide promoters (CeO_2, Ga_2O_3, La_2O_3, MnO, MgO, *etc.*) were adopted, and the positive effects of them have also been documented [15–26]. Additionally, the composition, texture of catalysts, and dispersion of metal and oxide phases on the catalysts are also greatly associated with their activities, which can be obtained using a variety of preparation methods [16,23,27–31] Arena *et al.* [16,21,28,32] used reverse co-precipitation under ultrasound irradiation to obtain a series of Cu-ZnO/ZrO_2 catalysts with a remarkable total surface area and high dispersion. Deng *et al.* [7,12] and Bonura *et al.* [32] adopted the oxalate-co-precipitated technique to enhance the catalyst activity, whereas Guo *et al.* [29,33] found that the combustion method was a simple, fast, and valuable route. The citrate method was also an important method for preparing CZZ catalysts investigated by Karelovic *et al.* [34]. It is known that the citrate method provides solids with high surface areas at relatively low calcination temperatures [20,21,34]. In addition, a homogeneous gel (containing the metal precursors) could be formed by complexing dissolved nitrate salts with citric acid consisting in the initial formation. However, it is no wonder that this field is still experiencing a renaissance with many new insights into the structural and functional properties of such CZZ systems, especially the mechanism of methanol formation from CO_2 and the role of different promoters acted during the hydrogenation process [16,18,20,35–37].

In this paper, a series of $CuO/ZnO/ZrO_2$ catalysts were prepared through the citrate method. The effects of the CuO/ZnO weight ratio on the structure and adsorption properties were systematically conducted, with a constant zirconia loading of 10 wt. %. In particular, the role of surface components on the optimum composition was investigated. According to the results, this study confirms that there is a synergetic effect existed in di/or multi-metal-oxide systems in detail of the physicochemical

characterization, which greatly change the adsorption properties of two reactants (CO_2 and H_2) during the hydrogenation process, leading to the different reaction activity for synthesizing MeOH from pure CO_2.

2. Results and Discussion

2.1. Textural Properties of CZZ Catalysts

The data of BET surface area (S_{BET}), pore volume (V_P) and CuO particle size are summarized in Table 1. It could be found that sample CZZ-271 exhibits the highest surface area of 81.8 $m^2 \cdot g^{-1}$ and pore volume of 0.31 $cm^3 \cdot g^{-1}$. With increasing Cu/Zn ratio, the surface area significantly decreased and finally reached to 41.2 $cm^3 \cdot g^{-1}$ of CZZ-721. A similar trend is also observed in pore volume data from BET and the diameter of CuO. The decrease of surface area and pore volume suggested that the increasing of Cu/Zn ratio signals a negative influence of the textural properties on the calcined CZZ catalysts, especially to the surface area. The growth of crystal grain and/or agglomeration of particles with the increase of Cu/Zn ratio should be responsible for the change of S_{BET} and V_P. The composition of CZZ catalysts (Table 1) confirm that the composition of final catalyst can be controlled exactly by the citrate complex decomposition method, although the ZnO contents were a little below the designed values.

Table 1. Physicochemical properties of different calcined CZZ catalysts.

Sample	Chemical Composition [a] (wt. %)			Cu:Zn	S_{BET}	V_P	CuO [b] Dia.
	CuO	ZnO	ZrO_2	(Atomic)	($m^2 \cdot g^{-1}$)	($cm^3 \cdot g^{-1}$)	(nm)
CZZ-271	21.5	67.0	11.5	0.3	81.8	0.31	10.3
CZZ-361	31.0	57.7	11.3	0.5	70.1	0.22	12.6
CZZ-451	41.2	48.6	11.7	0.8	61.6	0.24	13.4
CZZ-541	52.0	37.7	10.3	1.3	48.3	0.27	14.0
CZZ-631	60.8	28.2	11.0	2.0	44.6	0.26	14.7
CZZ-721	70.4	18.8	10.8	3.6	41.2	0.16	16.2

[a] Values measured by ICP; [b] Calculated by Scherrer formula.

The XRD patterns of the calcined CZZ samples with different Cu/Zn weight ratios are shown in Figure 1. It is observed that several diffraction peaks appear at 2θ of 32.4°, 35.4°, 38.7°, indicating the presence of the CuO phase, while the peaks account for crystalline ZnO (2θ = 31.8°, 34.5°, 36.3°), which are partly overlapping with each other, are also detectable for all of the samples. Noticeably, with the increase of Cu/Zn ratio, the diffraction peaks of CuO become stronger and sharper, while the peaks attributed to ZnO have the opposite variation trend. In sample CZZ-271, only a small band is observed at 38.7°, indicating the highest dispersion of the CuO domains. The crystal size of CuO particles, which are estimated using the Scherrer equation, increase from 10.3 nm of CZZ-271 to 16.2 nm of CZZ-721, as shown in Table 1. No diffraction peak of the ZrO_2 phase can be detected, showing that the ZrO_2 crystals are fine and highly dispersed.

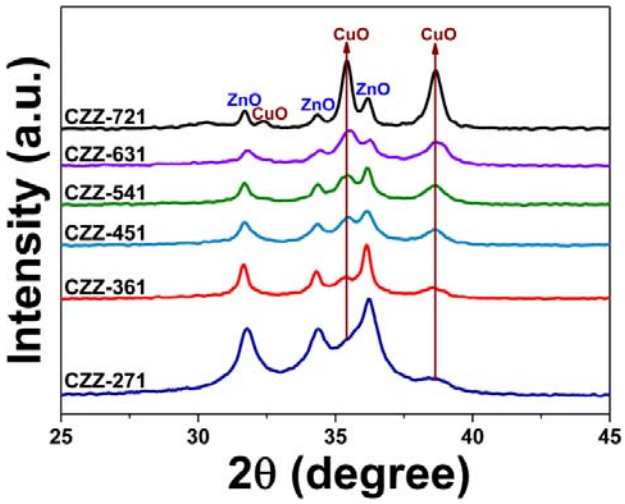

Figure 1. XRD patterns of calcined catalysts.

2.2. Reduction Behaviour of CZZ Catalysts

In order to investigate the reduction behaviour of such catalysts, H_2-TPR measurement was carried out, and the corresponding profiles are shown in Figure 2. Since ZnO and ZrO_2 cannot be reduced within this temperature range, those peaks and bands can be attributed to the reduction of the CuO phase.

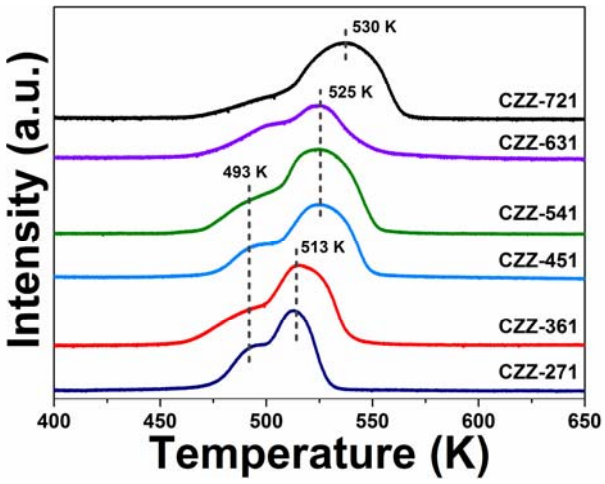

Figure 2. H_2-TPR profiles of calcined catalysts.

It is interesting to find two peaks of H_2 consumption for CZZ-271, which clearly shows that there are two types of CuO phases existing in two such samples. The low temperature peak is attributed to highly dispersed CuO particles, whereas the peak located at high temperature is due to the reduction of bulk CuO or composite metal oxide [38]. Obviously, with a gradual increase of Cu content, the low temperature peaks become a slope, as shown in CZZ-361, 451, 541, and 631 and, finally, there is only a broad band in CZZ-721, while the peak area becomes much larger and shifts towards the higher range. This trend could correspond to the growth of CuO diameter, shown in Table 1. With the increase of the Cu/Zn ratio, two kinds of CuO particles (highly dispersed and bulk ones) both gradually

grow and finally overlap with each other, leading to the changes of H_2 reduction behaviors of CZZ catalysts.

2.3. Morphologies of Catalysts

The morphologies of different calcined CZZ samples are shown in Figure 3. It is possible to observe the existence of cavities over all of the catalyst texture, seemly originated by citrate decomposition, combining with the increasing trend of caking with the increase of the Cu/Zn ratio.

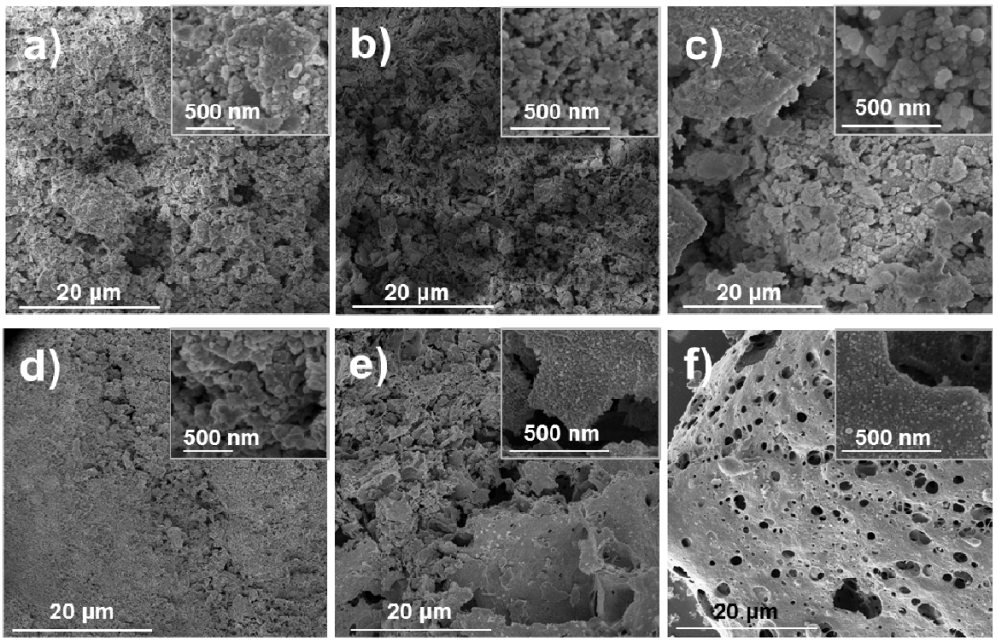

Figure 3. SEM images of calcined catalysts. (**a**) CZZ-271; (**b**) CZZ-361; (**c**) CZZ-451; (**d**) CZZ-541; (**e**) CZZ-631; and (**f**) CZZ-721.

An enlarged SEM image (Figure 3a) from the surface of the catalyst reveals that CZZ-271 was composed of numerous nanoparticles. In addition, the nanoparticles, which are looking like the loose cakes, can also be found in CZZ-361 (Figure 3b). It is well known that the increased Cu/Zn weight ratio leads to the agglomeration of nanoparticle, and such a phenomenon can be observed in CZZ-451 (Figure 3c) and CZZ-541 (Figure 3d) catalysts. Finally, with a yet higher Cu/Zn ratio (Figure 3e,f) the individual nanoparticles could not be found and an agglomerate of nanoparticles inlayed on a sinter plate-like structure was observed.

2.4. H_2 Chemisorption

To understand the adsorption properties of H_2 on different reduced CZZ catalysts, H_2-TPD study was performed for those pre-reduced CZZ catalysts. As shown in Figure 4, all the reduced CZZ catalysts display a similar desorption pattern, demonstrating that there are two adsorptive forms on the surfaces. According to the literature, the resolved peak (peak α) at low temperature (390–480 K) is attributed to the desorption of atomic hydrogen on Cu sites [39], while the much broader peak (peak β) located at 650 K represents the desorption of strongly-adsorbed hydrogen either on the surface of bulk Cu particles or other metal oxides surfaces, respectively [39–42]. From the data of peak α, it is found

that the amount of H_2 desorption decreases slowly with the increase of the Cu/Zn ratio, which might be attributed to the loss of surface area, and it maintains nearly the same value at high temperature.

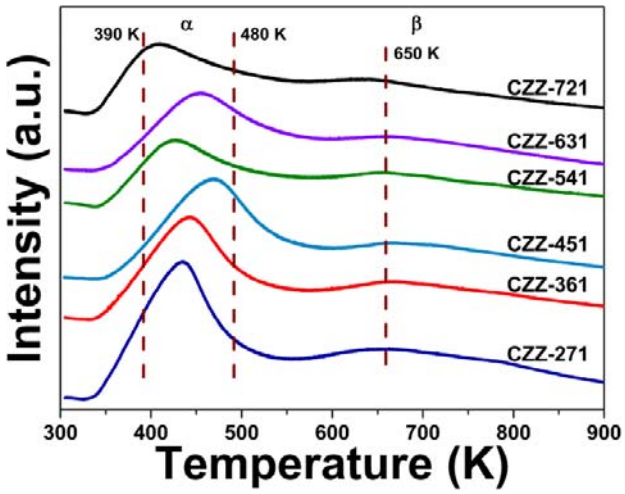

Figure 4. H_2-TPD curves of pre-reduced catalysts.

2.5. CO_2 Chemisorption and XPS Analysis

CO_2-TPD study of different CZZ catalysts was performed after pre-reduction, with the purpose of understanding the stability of CO_2 adsorbed and stored on the surface. In Figure 5, two peaks are observed in all the samples (denoted as α and β), representing two different adsorptive forms, in which peak groups α and β are related to the linear adsorptive and bridge adsorptive forms, respectively [43]. Peak group α appears in low temperature range (between 350 and 454 K) while peak group β locates in high temperature range (between 640 and 680 K), showing the easier desorption for the former and more difficult desorption for the later.

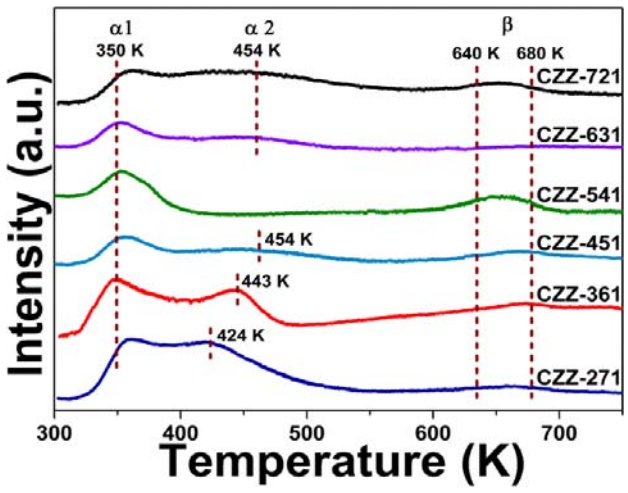

Figure 5. CO_2-TPD curves of pre-reduced catalysts.

For peak group α, peaks of the weakly basic sites (located at 350 K, donated as α1) are ascribed to surface hydroxyl groups, while the moderately basic site peaks (located at 420–450 K, donated as α2) are related to metal-oxygen pairs (such as Zn-O, Zr-O, M-O) [44]. As shown in Figure 5, the peak α1

areas of CZZ-271 and CZZ-361 are larger than peak α1 in the other samples. With increasing Cu content, peak α2 shifted from 424 K (sample CZZ-271) to 454 K (sample CZZ-451), while the corresponding area of peak α2 totally disappeared in sample CZZ-541, whereas such peaks appeared again in samples CZZ-631 and 721, in which only a low band could be observed. Combining with the surface atomic concentrations, as shown in Table 2, we found that the contribution of medium basic sites (peak α2) is closely associated with the ZnO/ZrO_2 species. When the Cu/Zn ratio increases from 0.3 to 0.8, the diameter of CuO particle grows, and much more ZnO/ZrO_2 particles are covered and overlapped by CuO phase, leading to a significant decrease of moderately basic sites, which are even dismissed in sample CZZ-541 for it maintain the lowest surface content of Zn^{2+} and Zr^{4+}. Then, with the increasing Cu/Zn ratio, Zn^{2+} content on the surface is continually decreased, and Zr^{4+} content significantly increased, resulting in the reappearance of peak α2. In addition, the major desorption peaks α1 and α2 both fall well within the temperature range at which the reaction carried out, suggesting that such desorption sites may play crucial roles in determining the catalytic performance.

Table 2. Surface atomic concentrations of Cu^{2+}, Zn^{2+}, and Zr^{4+} in different CZZ catalysts.

Element	Surface Atomic Concentrations of Calcined Catalysts (at.%)					
	CZZ-271	**CZZ-361**	**CZZ-451**	**CZZ-541**	**CZZ-631**	**CZZ-721**
Cu^{2+}	4.2	5.7	13.0	13.2	14.9	19.6
Zn^{2+}	34.4	32.6	23.1	20.1	17.1	11.9
Zr^{4+}	5.6	5.8	3.9	3.6	6.3	7.0

Determined by XPS analysis.

2.6. Catalytic Performance of CO_2 into Methanol

The catalytic activity and selectivity of MeOH on all CZZ catalysts are listed in Table 3. CO and MeOH are the only carbon-containing products under the reaction conditions and traces of methane could be detected. It can be seen that sample CZZ-271 maintained the highest conversion (32.9%) and the WTY (193.9 $g \cdot kg^{-1} \cdot h^{-1}$). With an increased Cu/Zn ratio, a continued decline of catalytic activity from CZZ-271 to CZZ-451 is observed and reached to a minimum number for sample CZZ-541 (conversion of CO_2 is 28.5%, and selectivity of methanol is 29.7%), then the catalytic activity increased again and finally reaches 32.0% on sample CZZ-721. This trend is just in line with the result of CO_2-TPD analysis of the medium basic sites, showing that there is a close relationship between the changes of catalytic performance of CZZ catalysts and the exposure of ZnO/ZrO_2 species, and the high reaction activity of CZZ-271 should contribute to the combination of good CuO dispersion and suitable basic properties on the surface.

Table 3. The activities of methanol synthesis from CO_2 hydrogenation over CZZ catalysts.

Samples	CO_2 Conversion (%)	Selectivity (C-mol %)		WTY of MeOH ($g \cdot kg^{-1} \cdot h^{-1}$)
		MeOH	CO	
CZZ-271	32.9	45.8	54.2	193.9
CZZ-361	31.9	39.3	60.7	161.1
CZZ-451	30.7	33.2	66.8	138.2
CZZ-541	28.5	29.7	70.3	108.7
CZZ-631	30.4	30.3	69.7	118.3
CZZ-721	32.0	35.1	64.9	144.6

Reaction conditions: T = 513 K, P = 2.6 MPa, WHSV = 3600 h^{-1}, and CO_2/H_2 = 1/3 (molar ratio).

2.7. Discussion on the Synergetic Effect of CZZ Catalyst

In spite of the extensive literature of oxide-promoted Cu catalyst, the role of different components is still matter of debate [4,13,14,20]. In this context, trying to reveal whether there is a synergetic effect via the interaction between different components and how that influences the catalytic reaction, systematic TPD studies of single, di-, and multi-component systems involved in MeOH synthesis reaction were conducted. The samples were all fabricated by the citrate method and the composition of those di-component systems is inherited from CZZ-271 sample, which are ZnO/ZrO_2-071, CuO/ZnO-270, and CuO/ZrO_2-201. The desorption profiles of H_2 (Figure 6a,b) and CO_2 (Figure 6c,d) on those samples are shown in Figure 6, while the catalytic performances are listed in Table 4.

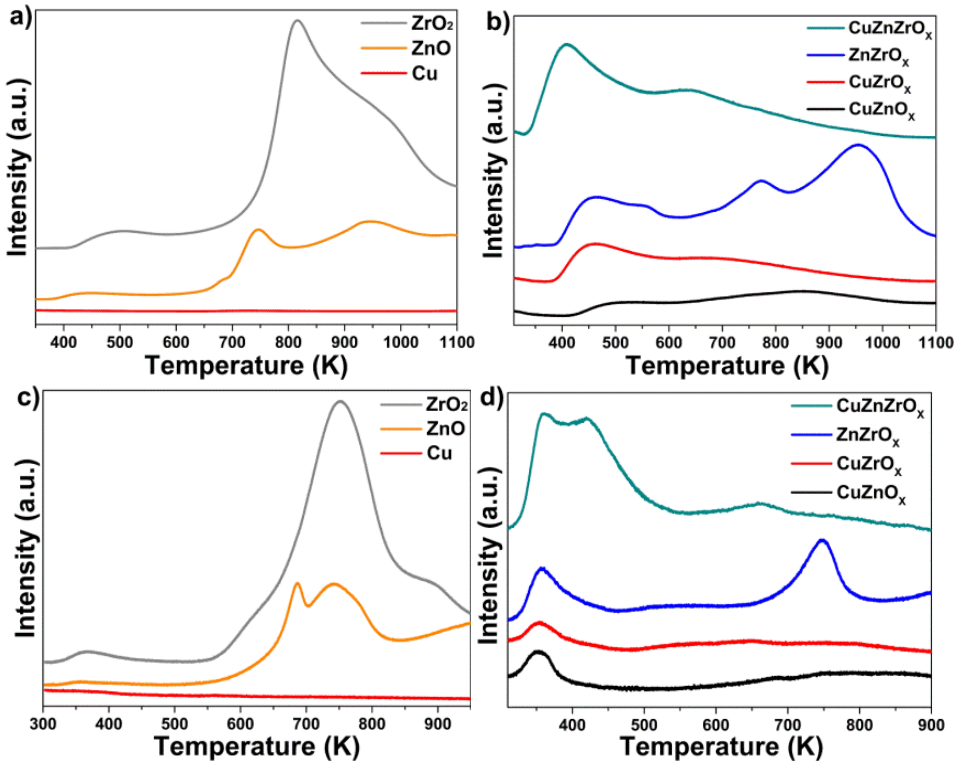

Figure 6. H_2-TPD profiles of (**a**) single component; (**b**) multi-components; and CO_2-TPD profiles of (**c**) single component; (**d**) multi-components.

Table 4. The activity of methanol synthesis from CO_2 hydrogenation over di-component CZZ systems.

Sample	CO_2 Conversion (%)	Selectivity (C-mol %)		WTY of MeOH ($g \cdot kg^{-1} \cdot h^{-1}$)
		MeOH	CO	
ZnO	1.5	-	100.0	-
ZrO_2	2.2	-	100.0	-
Cu [a]	6.3	28.8	71.2	23.4
ZnO/ZrO_2-071	3.3	-	100.0	-
Cu [a]/ZnO-270	28.3	29.8	70.2	108.2
Cu [a]/ZrO_2-201	22.7	31.9	68.1	93.3

Reaction conditions: T = 513 K, P = 2.6 MPa, WHSV = 3600 h^{-1}, and CO_2/H_2 = 1/3 (molar ratio). [a] Obtained from CuO after reduction.

As shown in Figure 6a, apart from the reduced Cu phase displaying no desorption peaks in the whole temperature range, the H_2-TPD pattern of single ZrO_2 and ZnO phases span a wide range of temperatures (400–1000 K), in which the main desorption peaks are all located at high temperature (above 750 K), while only small bands could be found in the low temperature range (400–550 K). This result clearly shows that no effective adsorption of H_2 happened on Cu surfaces, while the adsorbed H_2 has an intensive interaction with ZrO_2 and ZnO surfaces. Then, the TPD patterns for the di-component systems (Figure 6b) demonstrate great differences compared with those single ones. A remarkable decrease of high temperature peak is observed, following with an opposite trend of the low temperature peak. Since those TPD-profiles of di-component systems showing no similarities with the single ones, new adsorption sites must be formed in those di- component systems, and the interaction between different phases is responsible for those new sites, leading to a greatly-changed H_2 adsorption property on catalyst surfaces. A similar profile of CO_2-TPD, shown in Figure 6c,d, is also observed. Finally, for comparison, profiles of the activated CZZ-271 system are also listed, (labeled as $CuZnZrO_x$), as shown in Figure 6b,d. It contains the highest peak area in both the low temperature ranges of H_2 and CO_2, comparing with all the other systems, and a new peak located at 430 K is found in Figure 6d, attributing to the medium basic site.

The CO_2 hydrogenation data of single component is summarized in Table 4 in terms of CO_2 conversion and MeOH selectivity. No MeOH is detected on samples of ZnO and ZrO_2, and the conversion of CO_2 is only 1.5% and 2.2%, respectively. The single copper catalyst prepared by the citrate method shows a performance with 6.3% CO_2 conversion and 28.8% MeOH selectivity. These findings indicate that it is the copper component of the catalyst which effects the reaction CO_2 hydrogenation to MeOH. The low activity of single copper catalyst is probably due to the weak adsorption of H_2 and CO_2 on Cu surfaces, as shown in Figure 6a,c. The previous report indicated that the adsorption of H_2 on Cu surfaces is difficult, which can be attributed to the high activation barrier for H_2 dissociation on the metal [45]. Meanwhile, it is possible that, before temperature programming, the weakly-adsorbed CO_2 on copper surfaces might not be sufficiently dissociated into CO and O species [46,47]. As a result, less Cu atoms were partially oxidized on the catalyst surface, leading to no CO_2 molecules being strongly adsorbed on Cu surfaces. Therefore, no desorption peaks of CO_2 were observed throughout the TPD measurement in the single copper system. Since a single copper catalyst cannot give us the satisfactory results for hydrogenation of CO_2 to methanol, the CO_2 hydrogenation data of di-component systems are also investigated. As shown in Table 4, it is observed that the

di-component systems are more active than those single ones. Although ZnO/ZrO_2-071 catalysts still maintain no MeOH product, the conversion of CO_2 on CuO/ZnO-270 and CuO/ZrO_2-201 catalysts greatly increase to 28.3% and 22.7%, and the WTY of MeOH reach 108.2 $g \cdot kg^{-1} \cdot h^{-1}$ and 93.3 $g \cdot kg^{-1} \cdot h^{-1}$, respectively. These results further confirm that Cu is the active phase for forming MeOH in CZZ catalysts, and the high activities of CuO/ZnO-270 and CuO/ZrO_2-201 systems should be originated from both the increase of catalyst surface area and the effective adsorption of two reactants (H_2 and CO_2) on the surface. Finally, an enhanced activity of the CZZ-271 catalyst (32.9% of conversion and 45.8% of MeOH selectivity) is obtained, which is attributed to the appearance of medium basic sites according to the previous findings, combining with a relatively highly-adsorbed H_2 content at low temperature range. Comparing with the single component system (Cu, ZnO, and ZrO_2), synergetic effects may be in di/or multi-component systems, with the presentation of different performances.

With the purpose of finding direct evidence of the interaction via different components, HR-TEM and EDX investigations of calclined CZZ-271 were carried out (Figure 7). As shown in Figure 7d, it has been discovered that the core where the reaction happens is mainly constituted by CuO and ZnO phases, decorated by ZrO_2 crystal, where the diffraction plane (002) and (200) corresponds to CuO phase, (101) relative to ZnO phase, and (111) of ZrO_2 tetragonal phase is well distinguishable [48].

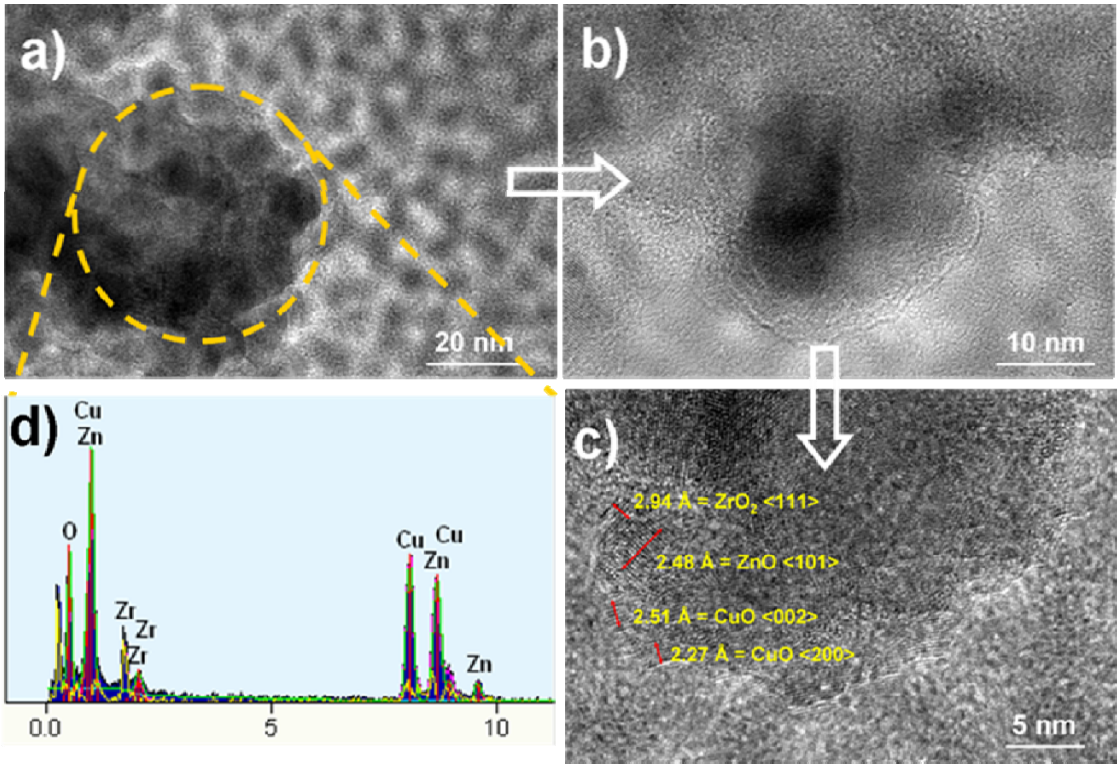

Figure 7. (**a**) TEM images of calcined CZZ-271 catalyst; (**b**) Enlarged TEM image of the catalyst; (**c**) The lattice planes of oxides and (**d**) EDX spectrum of calcined catalyst CZZ-271.

Combining with the results mentioned above, we determined that the adsorption properties of H_2 and CO_2 could be greatly influenced by the catalyst composition, leading to the different reaction activities. Furthermore, the CZZ-271 catalyst demonstrates a remarkable catalytic reactivity on CO_2

conversion to methanol for the suitable concentration of neighboring hydrogenation and CO_2-activated sites when the hydrogenation of CO_2 happened on Cu surfaces.

3. Experimental Section

3.1. Catalyst Preparation

In order to investigate the effect of chemical composition in CuO/ZnO/ZrO_2 system, five ternary catalysts with a constant zirconia loading (10 wt. %) and CuO/ZnO = 2/7, 3/6, 4/5, 5/4, 6/3, and 7/2 (labeled as CZZ-271, CZZ-361, CZZ-451, CZZ-541, CZZ-631, and CZZ-721, respectively) have been prepared by the citrate decomposition method. This method consists in the formation of a homogeneous gel (containing the metallic elements desired in the final catalyst) by complexing dissolved nitrates salts with citric acid. A homogeneous sol was formed by simultaneous adding an aqueous solution of citric acid (0.6 M) and an 0.5 M (the total cation concentration) aqueous solution containing the desired proportions of metal precursors, *i.e.*, $Cu(NO_3)_2{\cdot}3H_2O$ (AR reagent 99%), $Zn(NO_3)_2{\cdot}6H_2O$ (99%), $Zr(NO_3)_2{\cdot}5H_2O$ (>98%) to hot water. And then a clear blue complex was formed. The complex was constant stirred in a water bath at 333 K for 4 h, subsequently aged 2 h in air at room temperature subsequently. Afterward most of the water was removed in a rotary evaporator working at 333 K under vacuum, transforming the liquid into a very viscous fluid. The obtained material was further dried at 385 K which causes an important increasing volume overnight and become a kind of expanded blue spongy solid. Upon calcination in static air at 723 K for 4 h with a heating rate of 1 $K{\cdot}min^{-1}$ the dried material was converted into the oxides. Thereafter, the resultant powder was pressed (12 MPa), crushed, and sieved to obtain particles in the range of 20–40 mesh for catalytic test.

In addition, CuO, ZnO, and ZrO_2, dual-metallic oxides were also prepared, which are CuO/ZnO, CuO/ZrO_2, and ZnO/ZrO_2 catalysts with the mass ratio of 2/7, 2/1, and 7/1 (labeled as CuO/ZnO-270, CuO/ZrO_2-201, ZnO/ZrO_2-071, respectively). For comparison, single-metallic oxides CuO, ZnO, and ZrO_2 catalysts were prepared with the procedure described above.

3.2. Catalyst Characterizations

The metal oxide composition was analyzed by inductively-coupled plasma-atomic emission spectroscopy (ICP-AES; IRIS Intrepid, Thermo Fisher Scientific, Waltham, MA, USA). BET surface areas (S_{BET}), pore volume (V_P) of the oxide precursors were obtained by measuring the N_2 adsorption-desorption isotherms (AUTOSORB-1-MP, Quantachrome, Boynton Beach, FL, USA) at its boiling point (77 K). Before measurements, the samples were outgassed at 573 K under vacuum (2 h). X-ray diffraction (XRD) of powder samples were recorded on a D/max-2400 diffractometer (Rigaku Corporation, Tokyo, Japan) operating with Cu Kα radiation at 40 kV and 100 mA. The spectra were collected in the range of 2θ from 10° to 85° with a scan step of 0.02° min^{-1}. The Scherrer equation was used to calculate the size of crystallites. Temperature-programmed-reduction (H_2-TPR) measurements of the calcined catalysts were performed on a Chemisorptions Analyzer (FINESORB-3010A, FINETEC INSTRUMENTS, Hangzhou, China). Powdered samples (20–40 mesh, 50 mg) in a U-tube quartz reactors were purged with Ar (30 $mL{\cdot}min^{-1}$) at room temperature for 15 min and then reduced

at a flow of Ar-carried 10 vol % H_2/Ar (10 mL·min^{-1}). The experiments were carried out in the temperature range from 293 to 973 K with a linear heating rate of 10 K·min^{-1}. A thermal conductivity detector (TCD, FINETEC INSTRUMENTS, Hangzhou, China) was used to monitor the consumption of H_2. Carbon dioxide (or hydrogen) temperature-programmed-desorption (CO_2-TPD or H_2-TPD) were taken at 293 K using the above chemisorption analyzer. The catalyst (50 mg) was first reduced at 523 K in 10 vol % H_2 in Ar flow of 30 mL·min^{-1} for 2 h on the above apparatus. After cooling to room temperature, the catalyst was saturated with CO_2 (99.99%, purity) of 30 mL·min^{-1} for 40 min, then flushed with a helium stream (10 mL·min^{-1}, 20 min) to remove all physical adsorbed CO_2. Afterward, the examined sample was heated to 973 K in a rate of 10 K·min^{-1} under He flow (10 mL·min^{-1}), and the desorbed CO_2 was detected by the response of thermal conductivity detector. H_2-TPD was performed as that of CO_2-TPD, and difference was that the change of helium stream as a carrier gas instead of Ar. The X-ray photoelectron spectroscopy (XPS) measurements were recorded on ESCALAB MK II X-ray photoelectron spectrometer (VG Instruments, London, UK). Scanning electron microscopy (SEM) was performed on field emission scanning electron microscopy (FESEM, FEI, NOVA NanoSEM 450, FEI, Hillsboro, OR, USA) with an accelerating voltage of 3 kV. Specimens were prepared by chromium sputtering of catalyst samples deposited as powders on flat stubs. Transmission electron microscopy (TEM) was performed with a FEI TF30 microscope (FEI, Hillsboro, OR, USA) at 20 kV, which was equipped with an energy-dispersive X-ray (EDX).

3.3. Catalysis

The activity measurements for CO_2 hydrogenation were carried out in a fixed-bed continuous flow reactor (stainless steel tubular 10 mm i.d). The reaction bed consisted of 1 g of the catalyst diluted with quartz sand placed between two layers of the same quartz sand (20–40 mesh) in the reactor. Prior to each reaction, the catalyst was firstly activated with a flow containing 10 vol % H_2 balanced with N_2 at 523 K for 2 h. Thereafter, the temperature was decreased to 513 K and the catalyst was subsequently exposed to the reaction mixture H_2/CO_2 (3/1 in molar ratio), weight hourly space velocity (WHSV) of 3600 L·kg$_{cat}^{-1}$·h^{-1}, at 2.6 MPa. The outlet gas lines were heated electrically at 393 K to prevent condensation of water, methanol, and other hydrocarbons in products. The outlet stream was analyzed using a gas chromatograph equipped with a thermal conductivity detector (FULI, GC-9790, Porapak Q column, FULI, Wenling, China). CO_2 conversion and the carbon-based selectivity for MeOH and CO were obtained by an internal normalization method and mass-balance at steady-state conditions after 1 h of time on stream. The WTY of MeOH, which gave the amounts of MeOH produced per gram catalyst per hour, was defined using the equation $WTY_{MeOH} = (W_T \times X_{MeOH}) / (t \times m)$, where W_T was the total weight of MeOH and H_2O product (g); X_{MeOH} was the mass fraction of CH_3OH; t was the reaction time (h); and m was the weight of catalyst (kg). Similar evaluating methods had been described in detail in the previous literatures [20,37].

4. Conclusions

A series of CZZ catalysts for the hydrogenation of CO_2 to methanol have been synthesized through the citrate method, with the evaluation of how CuO/ZnO weight ratio affect the catalytic functionality and how ZnO and ZrO_2 influence the catalytic activity during the hydrogenation process. Results

showed that CuO/ZnO/ZrO_2-271 catalysts possessed the highest WTY of methanol from CO_2 hydrogenation, since it has the best CuO dispersion, good texture properties, and the highest content of medium basic sites. In addition, it was confirmed that there was a synergetic effect existing in di- or multi-metal-oxide systems. This effect could greatly change the low temperature adsorption properties of CO_2 and H_2 during the hydrogenation process, which leads to the different reaction activity for synthesizing methanol from pure CO_2.

Acknowledgments

The authors would like to thank the DUT Chemistry Analysis and Research Center and Zhanming Gao for the contributions on the material characterization.

Author Contributions

The experimental work was conceived and designed by C.H. and Y.Z.; S.C. and D.L. performed the experiments; C.H., X.F. and D.L. analyzed the data; C.H. and S.C. drafted the paper. The manuscript was amended through the comments of all authors. All authors have given approval for the final version of the manuscript.

Conflicts of Interest

The authors declare no conflict of interest.

References

1. Olah, G.A.; Prakash, G.K.S.; Goeppert, A. Anthropogenic chemical carbon cycle for a sustainable future. *J. Am. Chem. Soc.* **2011**, *133*, 12881–12898.
2. Zangeneh, F.T.; Sahebdelfar, S.; Ravanchi, M.T. Conversion of carbon dioxide to valuable petrochemicals: An approach to clean development mechanism. *J. Nat. Gas Chem.* **2011**, *20*, 219–231.
3. Olah, G. After oil and gas: Methanol economy. *Catal. Lett.* **2004**, *93*, 1–2.
4. Nakamura, J.; Uchijima, T.; Kanai, Y.; Fujitani, T. The role of ZnO in Cu/ZnO methanol synthesis catalysts. *Catal. Today* **1996**, *28*, 223–230.
5. Behrens, M. Heterogeneous catalysis of CO_2 conversion to methanol on copper surfaces. *Angew. Chem. Int. Ed.* **2014**, *53*, 12022–12024.
6. Inui, T.; Hara, H.; Takeguchi, T.; Kim, J. Structure and function of Cu-based composite catalysts for highly effective synthesis of methanol by hydrogenation of CO_2 and CO. *Catal. Today* **1997**, *36*, 25–32.
7. Ma, Y.; Sun, Q.; Wu, D.; Fan, W.; Zhang, Y.; Deng, J. A practical approach for the preparation of high activity Cu/ZnO/ZrO_2 catalyst for methanol synthesis from CO_2 hydrogenation. *Appl. Catal. A* **1998**, *171*, 45–55.
8. Saito, M. R & D activities in Japan on methanol synthesis from CO_2 and H_2. *Catal. Surv. Jpn.* **1998**, *2*, 175–184.

9. Saito, M.; Fujitani, T.; Takeuchi, M.; Watanabe, T. Development of copper/zinc oxide-based multicomponent catalysts for methanol synthesis from carbon dioxide and hydrogen. *Appl. Catal. A* **1996**, *138*, 311–318.
10. Melián-Cabrera, I.; López-Granados, M.; Fierro, J.L.G. Reverse Topotactic Transformation of a Cu-Zn-Al Catalyst during Wet Pd Impregnation: Relevance for the Performance in Methanol Synthesis from CO_2/H_2 Mixtures. *J. Catal.* **2002**, *210*, 273–284.
11. Waugh, K.C. Methanol Synthesis. *Catal. Today* **1992**, *15*, 51–75.
12. Sun, Q.; Liu, C.; Pan, W.; Zhu, Q.; Deng, J. *In situ* IR studies on the mechanism of methanol synthesis over an ultrafine $Cu/ZnO/Al_2O_3$ catalyst. *Appl. Catal. A* **1998**, *171*, 301–308.
13. Arena, F.; Mezzatesta, G.; Zafarana, G.; Trunfio, G.; Frusteri, F.; Spadaro, L. Effects of oxide carriers on surface functionality and process performance of the Cu-ZnO system in the synthesis of methanol via CO_2 hydrogenation. *J. Catal.* **2013**, *300*, 141–151.
14. Sato, A.G.; Volanti, D.P.; Meira, D.M.; Damyanova, S.; Longo, E.; Bueno, J.M.C. Effect of the ZrO_2 phase on the structure and behavior of supported Cu catalysts for ethanol conversion. *J. Catal.* **2013**, *307*, 1–17.
15. Raudaskoski, R.; Marita, V.N.; Keiski, R.L. The effect of ageing time on co-precipitated $CuZnOZrO_2$ catalysts used in methanol synthesis from CO_2 and H_2. *Top. Catal.* **2007**, *45*, 57–60.
16. Arena, F.; Katia, B.; Giuseppe, I.; Giuseppe, B.; Lorenzo, S.; Francesco, F. Synthesis, characterization and activity pattern of $Cu-ZnO/ZrO_2$ catalysts in the hydrogenation of carbon dioxide to methanol. *J. Catal.* **2007**, *249*, 185–194.
17. Natesakhawat, S.; Lekse, J.W.; Baltrus, J.P.; Ohodnicki, P.R.; Howard, B.H.; Deng, X.; Matranga, C. Active Sites and Structure—Activity Relationships of Copper-Based Catalysts for Carbon Dioxide Hydrogenation to Methanol. *ACS Catal.* **2012**, *2*, 1667–1676.
18. Liao, F.; Zeng, Z.; Eley, C.; Lu, Q.; Hong, X.; Tsang, S.C.E. Electronic modulation of a copper/Zinc oxide catalyst by a heterojunction for selective hydrogenation of carbon dioxide to methanol. *Angew. Chem.* **2012**, *124*, 5934–5938.
19. Jia, L.; Gao, J.; Fang, W.; Li, Q. Influence of copper content on structural features and performance of pre-reduced $LaMn_{1-x}Cu_xO_3$ ($0 \leq x < 1$) catalysts for methanol synthesis from CO_2/H_2. *J. Rare Earth* **2010**, *28*, 747–751.
20. Słoczyński, J.; Grabowski, R.; Olszewski, P.; Kozłowska, A.; Stoch, J.; Lachowska, M.; Skrzypek, J. Effect of metal oxide additives on the activity and stability of $Cu/ZnO/ZrO_2$ catalysts in the synthesis of methanol from CO_2 and H_2. *Appl. Catal. A* **2006**, *310*, 127–137.
21. Słoczyński, J.; Grabowski, R.; Kozłowska, A.; Olszewski, P.; Lachowska, M.; Skrzypek, J.; Stoch, J. Effect of Mg and Mn oxide additions on structural and adsorptive properties of $Cu/ZnO/ZrO_2$ catalysts for the methanol synthesis from CO_2. *Appl. Catal. A* **2003**, *249*, 129–138.
22. Brown, N.J.; Weiner, J.; Hellgardt, K.; Shaffer, M.S.P.; Williams, C.K. Phosphinate stabilised ZnO and Cu colloidal nanocatalysts for CO_2 hydrogenation to methanol. *Chem. Commun.* **2013**, *49*, 11074–11076.
23. Bonura, G.; Arena, F.; Mezzatesta, G.; Cannilla, C.; Spadaro, L.; Frusteri, F. Role of the ceria promoter and carrier on the functionality of Cu-based catalysts in the CO_2-to-methanol hydrogenation reaction. *Catal. Today* **2011**, *171*, 251–256.

24. Wang, L.; Liu, Q.; Chen, M.; Liu, Y.; Cao, Y.; He, H.; Fan, K. Structural Evolution and Catalytic Properties of Nanostructured Cu/ZrO_2 Catalysts Prepared by Oxalate Gel-Coprecipitation Technique. *J. Phys. Chem. C* **2007**, *111*, 16549–16557.
25. Ladera, R.; Pérez-Alonso, F.J.; González-Carballo, J.M.; Ojeda, M.; Rojas, S.; Fierro, J.L.G. Catalytic valorization of CO_2 via methanol synthesis with Ga-promoted Cu-ZnO-ZrO_2 catalysts. *Appl. Catal. B* **2013**, *142–143*, 241–248.
26. Liao, F.; Huang, Y.; Ge, J.; Zheng, W.; Tedsree, K.; Collier, P.; Hong, X.; Tsang, S.C. Morphology-dependent interactions of ZnO with Cu nanoparticles at the materials' interface in selective hydrogenation of CO_2 to CH_3OH. *Angew. Chem. Int. Ed.* **2011**, *50*, 2162–2165.
27. Yang, C.; Ma, Z.; Zhao, N.; Wei, W.; Hu, T.; Sun, Y. Methanol synthesis from CO_2-rich syngas over a ZrO_2 doped CuZnO catalyst. *Catal. Today* **2006**, *115*, 222–227.
28. Arena, F.; Italiano, G.; Barbera, K.; Bonura, G.; Spadaro, L.; Frusteri, F. Basic evidences for methanol-synthesis catalyst design. *Catal. Today* **2009**, *143*, 80–85.
29. Guo, X.; Mao, D.; Lu, G.; Wang, S.; Wu, G. Glycine-nitrate combustion synthesis of CuO-ZnO-ZrO_2 catalysts for methanol synthesis from CO_2 hydrogenation. *J. Catal.* **2010**, *271*, 178–185.
30. Liu, X.; Lu, G.Q.; Yan, Z.; Beltramini, J. Recent Advances in Catalysts for Methanol Synthesis via Hydrogenation of CO and CO_2. *Ind. Eng. Chem. Res.* **2003**, *42*, 6518–6530.
31. Zhang, Y.; Fei, J.; Yu, Y.; Zheng, X. Methanol synthesis from CO_2 hydrogenation over Cu based catalyst supported on zirconia modified γ-Al_2O_3. *Energy Convers. Manag.* **2006**, *47*, 3360–3367.
32. Bonura, G.; Cordaro, M.; Cannilla, C.; Arena, F.; Frusteri, F. The changing nature of the active site of Cu-Zn-Zr catalysts for the CO_2 hydrogenation reaction to methanol. *Appl. Catal. B* **2014**, *152–153*, 152–161.
33. Guo, X.; Mao, D.; Wang, S.; Wu, G.; Lu, G. Combustion synthesis of CuO-ZnO-ZrO_2 catalysts for the hydrogenation of carbon dioxide to methanol. *Catal. Commun.* **2009**, *10*, 1661–1664.
34. Karelovic, A.; Bargibant, A.; Fernández, C.; Ruiz, P. Effect of the structural and morphological properties of Cu/ZnO catalysts prepared by citrate method on their activity toward methanol synthesis from CO_2 and H_2 under mild reaction conditions. *Catal. Today* **2012**, *197*, 109–118.
35. Słoczyński, J.; Grabowski, R.; Kozłowska, A.; Olszewski, P.; Stoch, J.; Skrzypek, J.; Lachowska, M. Catalytic activity of the M/($3ZnO{\cdot}ZrO_2$) system (M = Cu, Ag, Au) in the hydrogenation of CO_2 to methanol. *Appl. Catal. A* **2004**, *278*, 11–23.
36. Kanai, Y.; Watanabe, T.; Fujitani, T.; Uchijima, T.; Nakamura, J. The synergy between Cu and ZnO in methanol synthesis catalysts. *Catal. Lett.* **1996**, *38*, 157–163.
37. Askgaard, T.S.; Norskov, J.K.; Ovesen, C.V.; Stoltze, P. A Kinetic Model of Methanol Synthesis. *J. Catal.* **1995**, *156*, 229–242.
38. Morikawa, M.; Ahmed, N.; Yoshida, Y.; Izumi, Y. Photoconversion of carbon dioxide in zinc-copper-gallium layered double hydroxides: The kinetics to hydrogen carbonate and further to CO/methanol. *Appl. Catal. B* **2014**, *144*, 561–569.
39. Dong, X.; Zhang, H.; Lin, G.; Yuan, Y.; Tsai, K.R. Highly Active CNT-Promoted Cu-ZnO-Al_2O_3 Catalyst for Methanol Synthesis from H_2/CO/CO_2. *Catal. Lett.* **2003**, *85*, 237–246.
40. Genger, T.; Hinrichsen, O.; Muhler, M. The temperature-programmed desorption of hydrogen from copper surfaces. *Catal. Lett.* **1999**, *59*, 137–141.

41. Ahlers, J.; Grasser, J.; Loveless, B.; Muggli, D. Room-temperature oxidation of reduced Cu/ZnO surfaces by lattice oxygen diffusion. *Catal. Lett.* **2007**, *114*, 185–191.
42. Wilmer, H.; Genger, T.; Hinrichsen, O. The interaction of hydrogen with alumina-supported copper catalysts: A temperature-programmed adsorption/temperature-programmed desorption/isotopic exchange reaction study. *J. Catal.* **2003**, *215*, 188–198.
43. Tao, J.; Zhang, W.; Chen, M.; Au, C.T. TPD and TPSR studies of CO_2 adsorption on Cu-baseed catalysts. *Nat. Gas Chem. Ind*. **1998**, *23*, 14–17.
44. Gao, P.; Li, F.; Zhao, N.; Xiao, F.; Wei, W.; Zhong, L.; Sun, Y. Influence of modifier (Mn, La, Ce, Zr and Y) on the performance of Cu/Zn/Al catalysts via hydrotalcite-like precursors for CO_2 hydrogenation to methanol. *Appl. Catal. A* **2013**, *468*, 442–452.
45. Sun, Q.; Xie, J.; Zhang, T. Dissociated adsorption of H_2 on surfaces of Ni Pd and Cu. *Acta Phys. Sin.* **1995**, *44*, 1805–1813.
46. Chinchen, G.C.; Spencer, M.S.; Waugh, K.C.; Whan, D.A. Promotion of methanol synthesis and the water-gas shift reactions by adsorbed oxygen on supported copper catalysts. *Faraday Trans. 1* **1987**, *83*, 2193–2212.
47. Hadden, R.A.; Vandervell, H.D.; Waugh, K.C.; Webb, G. The adsorption and decomposition of carbon dioxide on polycrystalline copper. *Catal. Lett.* **1988**, *1*, 27–33.
48. Bonura, G.; Cordaro, M.; Spadaro, L.; Cannilla, C.; Arena, F.; Frusteri, F. Hybrid Cu-ZnO-ZrO_2/H-ZSM5 system for the direct synthesis of DME by CO_2 hydrogenation. *Appl. Catal. B* **2013**, *140–141*, 16–24.

© 2015 by the authors; licensee MDPI, Basel, Switzerland. This article is an open access article distributed under the terms and conditions of the Creative Commons Attribution license (http://creativecommons.org/licenses/by/4.0/).